Boletim da Sociedade Astronômica Brasileira, **30**, no. 1, 128-131

Intermediate-mass black holes in dwarf galaxies at high redshifts

Paramita Barai & Elisabete M. de Gouveia Dal Pino

[1] Instituto de Astronomia, Geofísica e Ciências Atmosféricas (IAG-USP), Universidade de São Paulo. e-mail: paramita.barai@iag.usp.br

Abstract. Black holes are mostly observed to be of stellar-mass or supermassive. By natural extension, there should be a population of Intermediate-Mass Black Holes (IMBHs: with mass between 100 to $10^6 M_\odot$) in the Universe; which has started to being observed currently. An exciting claim has been made recently by Silk (2017): that there are IMBHs in essentially all old Dwarf Galaxies. Early feedback by IMBHs in gas-rich dwarf galaxies at $z = 5 - 8$, can potentially solve multiple dwarf galaxy problems (e.g. core-cusp, number) within the Λ-cold-dark-matter cosmology. Here we perform cosmological hydrodynamical simulations to test the case for IMBHs in Dwarf Galaxies. Our simulations employ the 3D TreePM SPH code GADGET-3, and include metal cooling, star formation, chemical enrichment, supernova feedback, AGN accretion and feedback. We are simulating small $(2\ \mathrm{Mpc})^3$ cosmological volumes with periodic boundary conditions, starting from $z = 100$. Black Holes of mass $10^2 - 10^3 M_\odot$ are seeded inside halos when they reach a mass of $10^6 - 10^7 M_\odot$. The black holes grow by accretion of gas from their surroundings and by merger with other black holes, and consequently eject feedback energy. By analyzing the simulation output in post-processing, we study the growth of the first IMBHs, and quantify the impact of IMBHs on star formation.

Resumo. Os buracos negros são observados principalmente como sendo de massa estelar ou supermassivos. Assim, naturalmente, deve haver no Universo uma população de Buracos Negros de massa-intermediária (IMBHs, Intermediate-Mass Black Holes) com massas entre 100 a $10^6 M_\odot$, que de fato tem sido observada atualmente. Uma importante afirmação foi realizada recentemente por Silk (2017): a de que IMBHs estão presentes, essencialmente, em todas as galáxias anãs mais velhas. O feedback inicial de IMBHs em galáxias anãs ricas em gás (em $z = 5 - 8$) pode potencialmente resolver múltiplos problemas de galáxias anãs (por exemplo, core-cusp, número) dentro da cosmologia ΛCDM. Neste trabalho, realizamos simulações hidrodinâmicas cosmológicas para testar a presença de IMBHs em galáxias anãs. Nossas simulações empregam o uso do código 3D TreePM SPH GADGET-3, e incluem o resfriamento de metais, a formação de estrelas, o enriquecimento químico, o feedback de supernovas, e a acreção e o feedback em AGNs. Estamos simulando pequenos volumes cosmológicos de $(2Mpc)^3$ com condições de fronteira periódicas, a partir de $z = 100$. Buracos Negros com massas entre $10^2 - 10^3 M_{odot}$ são semeados dentro de halos quando estes atingem uma massa entre $10^6 - 10^7 M_\odot$. Os buracos negros crescem pela acreção de gás ao redor deles e por fusão com outros buracos negros que, conseqüentemente, ejetam energia por feedback. Ao analisar os dados das simulações no pós-processamento, estudamos o crescimento das primeiras IMBHs e quantificamos o impacto da IMBH na formação de estrelas.

Keywords. cosmology: theory – black holes – dwarf galaxies

1. Introduction

Black holes usually come in two flavours: stellar-mass ($M_{\rm BH} \leq 10 M_\odot$), and supermassive ($M_{\rm BH} \geq 10^6 M_\odot$). Naturally, there should be a population of Intermediate-Mass Black Holes (IMBHs) of masses between $100 - 10^6 M_\odot$. Analogous to supermassive BHs producing AGN feedback, the IMBHs should also have feedback. Energy radiated by BHs affect their host galaxies, and drives galactic outflows. In this work we focus on negative BH feedback effects where star-formation is quenched.

AGN feedback mechanism has recently started to been observed in low-mass galaxies. Investigating the presence of AGN in nearby dwarf galaxies using mid-infrared emission, Marleau et al. (2017) identified 303 candidates, of which 91% were subsequently confirmed as AGN by other methods. The stellar masses of these galaxies are estimated to be between $10^6 - 10^9 M_\odot$; and the black hole masses in the range $10^3 - 10^6 M_\odot$. Penny et al. (2017) presented observational evidence for AGN feedback in a sample of 69 quenched low-mass galaxies ($M_\star < 4 \times 10^9 M_\odot$); including 6 galaxies showing signatures of an active AGN preventing ongoing star-formation.

The concordance ΛCDM cosmological scenario of galaxy formation presents multiple challenges in the dwarf galaxy mass range: e.g. core-cusp, number of DGs. Recently, Silk (2017) made an exciting claim that the presence of IMBHs at the centers of essentially all old Dwarf Galaxies (DGs) can potentially solve the problems. Early feedback from these IMBHs output energy and affect the host gas-rich DGs at $z = 5 - 8$. This early feedback can quench star-formation, reduce the number of DGs, and impact the density profile at DG centers. Dashyan et al. (2017) studied the same problem analytically, and compared AGN versus SN feedback. They find a critical halo mass below which the central AGN can drive gas out of the host halo. This negative feedback effect of AGN is found to be more efficient than SN in the most massive DGs, where SN is not able to expel the gas.

In this work, we investigate the scenario that IMBHs are present at the centers of all dwarf galaxies, by performing cosmological hydrodynamical simulations. Our goals are to (i) test if IMBHs would grow at DG centers, and (ii) quantify the impact on star formation.

2. Numerical Method

We use a modified version of the TreePM (particle mesh) — SPH (smoothed particle hydrodynamics) code GADGET-3 (Springel , 2005).

Radiative cooling and heating is incorporated from Wiersma, Schaye & Smith (2009). Eleven element species (H, He, C, Ca, O, N, Ne, Mg, S, Si, Fe) are tracked. Star-formation is implemented following the multiphase effective sub-resolution model by Springel & Hernquist (2003). Stellar evolution and chem-

ical enrichment are computed for the 11 elements, and kinetic feedback from supernovae is included (Tornatore et al. , 2007).

2.1. BH Accretion and Feedback

BHs are collisionless sink particles (of mass $M_{\rm BH}$) in our simulations. A BH (of initial mass $M_{\rm BHseed}$) is seeded at the center of each galaxy more massive than a total mass $M_{\rm HaloMin}$, which does not contain a BH already. We test different values of minimum halo mass and seed BH mass in the range: $M_{\rm HaloMin} = (10^6 - 10^7)M_\odot$, and $M_{\rm BHseed} = (10^2 - 10^3)M_\odot$.

Gas is considered to accrete onto a BH according to the Bondi-Hoyle-Lyttleton accretion rate $\dot{M}_{\rm Bondi}$ (Hoyle & Lyttleton , 1939; Bondi , 1952), and is limited to the Eddington rate ($\dot{M}_{\rm Edd}$),

$$\dot{M}_{\rm BH} = \min\left(\dot{M}_{\rm Bondi}, \dot{M}_{\rm Edd}\right), \tag{1}$$

$$\dot{M}_{\rm Bondi} = \alpha \frac{4\pi G^2 M_{\rm BH}^2 \rho}{(c_s^2 + v^2)^{3/2}}, \tag{2}$$

where G is the gravitational constant, ρ is the gas density, c_s is the sound speed, and v is the velocity of the BH relative to the gas. We set $\alpha = 100$ as a numerical boost factor (Springel, Di Matteo & Hernquist , 2005). The Eddington luminosity is used to express the Eddington mass accretion rate,

$$L_{\rm Edd} = \frac{4\pi G M_{\rm BH} m_p c}{\sigma_T} = \epsilon_r \dot{M}_{\rm Edd} c^2, \tag{3}$$

where m_p is the mass of a proton, c is the speed of light, and σ_T is the Thomson scattering cross-section for an electron. A fraction of the accretion rest-mass energy is coupled to the surrounding gas as feedback energy:

$$\dot{E}_{\rm feed} = \epsilon_f \epsilon_r \dot{M}_{\rm BH} c^2. \tag{4}$$

Here ϵ_r is the radiative efficiency, and ϵ_f is the feedback efficiency. We adopt the mean value for radiatively efficient accretion onto a Schwarzschild BH (Shakura & Sunyaev , 1973): $\epsilon_r = 0.1$.

The BH feedback energy is distributed in the *kinetic* form (introduced in Barai et al. 2014, 2016). Surrounding gas is driven outward at a velocity v_w and mass outflow rate $\dot{M}_w$. Given energy conservation,

$$\frac{1}{2}\dot{M}_w v_w^2 = \dot{E}_{\rm feed}, \tag{5}$$

and using Eq. (4), the outflow rate can be expressed in terms of the BH accretion rate,

$$\dot{M}_w = 2\epsilon_f \epsilon_r \dot{M}_{\rm BH} \frac{c^2}{v_w^2}. \tag{6}$$

We use the values: $\epsilon_f = 0.05$, and $v_w = 2000$ km/s.

The implementation in the GADGET-3 code involves computing physical quantities by kernel-weighted smoothing over gas particles neighboring each BH. The kernel size, or the BH smoothing length $h_{\rm BH}$, is determined at each timestep by implicit solution of the equation,

$$\frac{4}{3}\pi h_{\rm BH}^3 \rho_{\rm BH} = M_{\rm ngb}, \tag{7}$$

where $\rho_{\rm BH}$ is the kernel estimate of the gas density at the position of the BH, and $M_{\rm ngb}$ is the mass of 200 neighboring gas particles.

In particular, the kinetic feedback energy from a BH is distributed to the surrounding gas lying inside a bi-cone volume. The slant height of each cone is $h_{\rm BH}$, and the half-opening angle is 45°. The cone-axis direction is considered as fixed for each BH, which is randomly assigned during a BH seeding. Gas particles lying within the bi-cone are tracked, and their total mass $M_{\rm gas}^{\rm vicinity}$ is computed. The probability for i-th gas particle within the bi-cone to be kicked is calculated:

$$p_i = \frac{\dot{M}_w \Delta t}{M_{\rm gas}^{\rm vicinity}}, \tag{8}$$

where Δt is the timestep, and $\dot{M}_w$ is the mass outflow rate obtained from Eq. (6). A random number x_i, uniformly distributed in the interval [0, 1], is drawn and compared with p_i. For $x_i < p_i$, the gas particle is given an AGN wind kick, such that its new velocity becomes:

$$\boldsymbol{v}_{\rm new} = \boldsymbol{v}_{\rm old} + v_w \hat{\boldsymbol{n}}. \tag{9}$$

The kick direction $\hat{n}$ is set radially outward from the BH.

We incorporate a scheme for BH *pinning*, or *BH advection algorithm* (also done in e.g., Schaye et al. 2015). Each BH is repositioned manually at each time-step to the center (minimum gravitational potential location) of its host galaxy. This is done in SPH simulations to correct for dynamical movements of BH particles wandering away from galaxy centers by numerical effects.

We consider that central BHs merge when their host galaxies merge during hierarchical structure formation. When two BH particles come near such that the distance between them is smaller than the smoothing length of either one, and their relative velocity is below the local sound speed, they are allowed to merge to form a single BH (Di Matteo et al. , 2012).

2.2. Simulations

We perform cosmological hydrodynamical simulations of small-sized boxes to probe dwarf galaxies at high redshifts. The initial condition at $z = 100$ is generated using the MUSIC[1] software (Hahn & Abel , 2011). A concordance flat ΛCDM model is used, with the cosmological parameters (Planck Collaboration (2015), results XIII): $\Omega_{M,0} = 0.3089, \Omega_{\Lambda,0} = 0.6911, \Omega_{B,0} = 0.0486, H_0 = 67.74$ km s^{-1} Mpc^{-1}.

The size of the cubic cosmological volume is $(2h^{-1}$ Mpc$)^3$ comoving. Hence the total mass of matter (dark matter + baryons) in the box is $6.86 \times 10^{11} h^{-1} M_\odot$. We use 256^3 dark matter and 256^3 gas particles in the initial condition. The dark matter particle mass is $m_{\rm DM} = 3.44 \times 10^4 h^{-1} M_\odot$, and the gas particle mass is $m_{\rm gas} = 6.43 \times 10^3 h^{-1} M_\odot$. The gravitational softening length is set to $L_{\rm soft} = 0.1 h^{-1}$ kpc comoving. Starting from $z = 100$, the box is subsequently evolved up to $z = 4$, with periodic boundary conditions.

We execute a series of 10 simulations, with characteristics listed in Table 1. All the 10 runs incorporate metal cooling, chemical enrichment, SF and SN feedback. The first run has no BH included, while the latter 9 explore different models of BH feedback.

Table 1. Simulation runs and parameters.

Run name	BH present	Min. Halo Mass for BH Seeding, $M_{\rm HaloMin}[M_\odot]$	Seed BH Mass, $M_{\rm BHseed}[M_\odot]$	BH kinetic feedback kick velocity v_w (km/s)
SN	No	–	–	–
BHs2h1e6	Yes	$h^{-1} \times 10^6$	10^2	2000
BHs2h7e7	Yes	$5h^{-1} \times 10^7$	10^2	2000
BHs3h1e7	Yes	1×10^7	10^3	2000
BHs3h2e7	Yes	2×10^7	10^3	2000
BHs3h3e7	Yes	3×10^7	10^3	2000
BHs3h4e7	Yes	4×10^7	10^3	2000
BHs3h4e7v5	Yes	4×10^7	10^3	5000
BHs3h5e7	Yes	5×10^7	10^3	2000
BHs4h4e7	Yes	4×10^7	10^4	2000

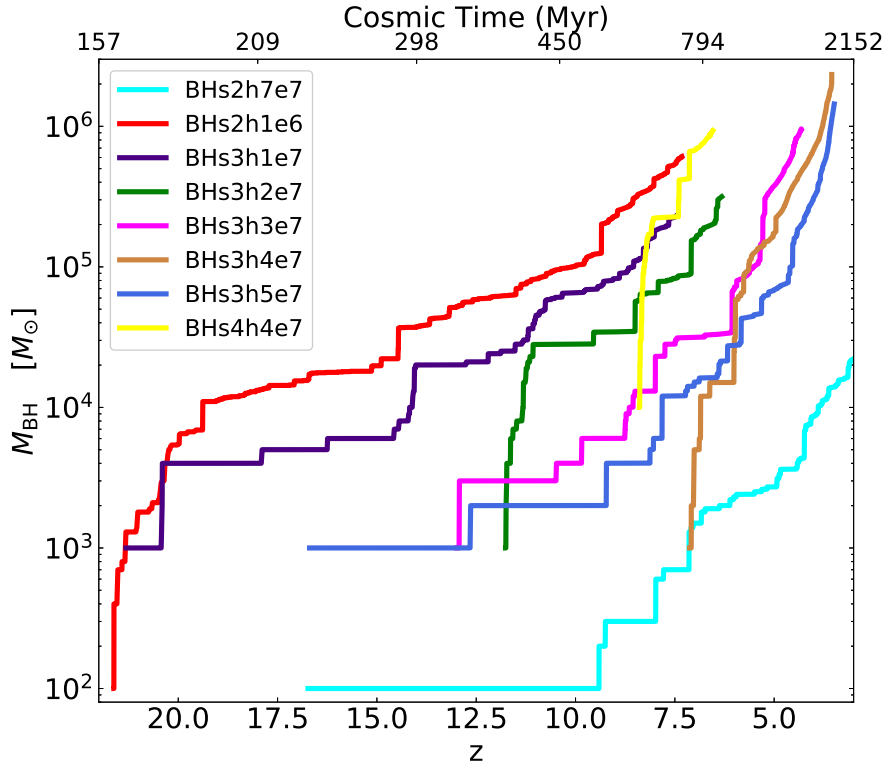

Figure 1. BH mass growth with redshift of the most-massive BH in each run. The different colours discriminate the runs.

3. Results and Discussion

3.1. Black Hole Accretion and Growth

We find that first BHs are seeded at different cosmic times depending on the value of minimum halo mass for BH seeding, $M_{\rm HaloMin}$. The seeding epoch varies between $z \sim 22$ to $z \sim 16$ in our simulations, when the first halos reach $M_{\rm halo} = h^{-1} \times 10^6 M_\odot$ to $M_{\rm halo} = 5 \times 10^7 M_\odot$. In the runs *BHs2h1e6*, *BHs2h7e7*, *BHs3h1e7* and *BHs3h5e7*, one of these first seeds grow to become the most-massive BH. However in runs *BHs3h2e7*, *BHs3h3e7*, *BHs3h4e7* and *BHs4h4e7*, the BH which becomes most-massive is seeded at later epochs $z \sim 11 - 7$. This variance in the seed epochs is because of the different BH growth modes.

The redshift evolution of the most-massive BH mass in the BH runs is plotted in Fig. 1. Each BH starts from an initial seed of $M_{\rm BH} = 10^2 M_\odot$ in the runs named *BHs2**, $10^3 M_\odot$ in the runs named *BHs3**, and $10^4 M_\odot$ in the runs named *BHs4**. The subsequent mass growth is due to merger with other BHs (revealed as vertical rises in $M_{\rm BH}$), and gas accretion (visualized as the positive-sloped regions of the $M_{\rm BH}$ versus z curve).

The final properties reached depends on the simulation. The most-massive BH, considering all the runs, has grown to $M_{\rm BH} = 2 \times 10^6 M_\odot$ at $z = 5$ in run *BHs3h4e7* (brown curve in Fig. 1).

3.2. Star Formation

Stars form in the simulation volume from cold dense gas. The Star Formation Rate Density (SFRD in units of $M_\odot yr^{-1} Mpc^{-3}$, counting stars forming in the whole simulation box) versus redshift of the simulation runs is displayed in Fig. 2. We take the *SN* run without BHs as the standard, and compare the *BH** runs with it to estimate the impact of BH feedback in star-formation.

The SFRD rises with time in the *SN* run (blue curve in Fig. 2) initially from $z \sim 15$, reaches a peak at $z \sim 4$ (the peak epoch

[1] MUSIC — Multi-scale Initial Conditions for Cosmological Simulations: https://bitbucket.org/ohahn/music

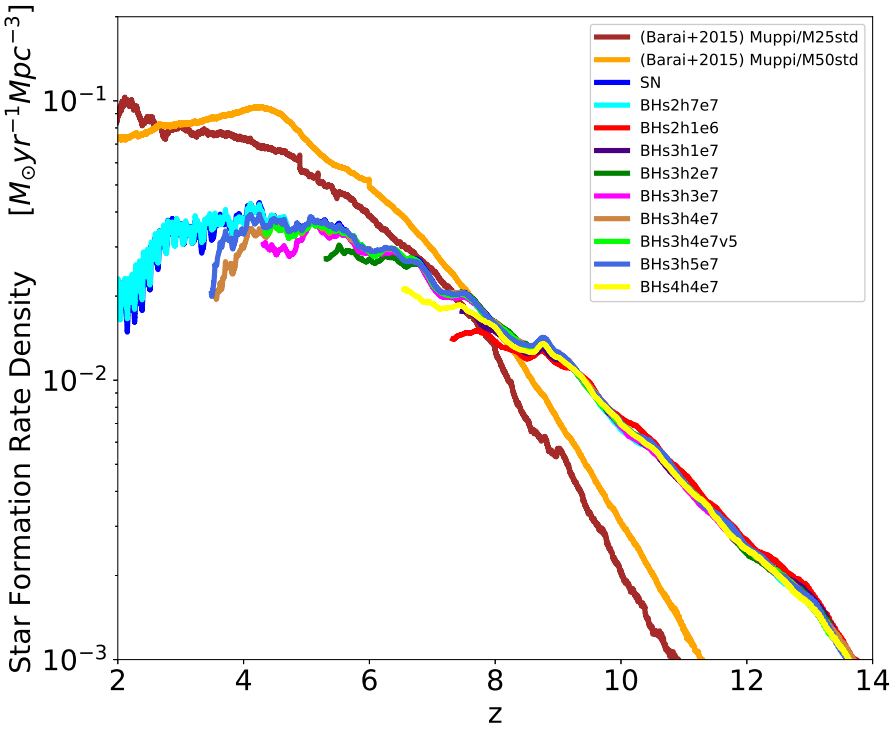

Figure 2. Total star formation rate density in simulation volume as a function of redshift.

of star-formation activity in the Universe), and decreases subsequently over $z \sim 4-2$. The SFRD in run *BHs2h7e7* (cyan curve) is almost similar to that in the run *SN*, because the BHs are too small there to generate enough feedback. A similar outcome happens in all the other runs at $z \geq 8$, when the BHs are too small.

The star-formation mostly occurs over an extended region at galaxy centers, where cosmic large-scale-structure gas inflows and cools. The presence of a BH quenches star formation by accreting some gas in, ejecting some gas out of the halo as outflows, and/or heating the gas.

The models suppress SF substantially from $z \sim 8$ onwards, when the BHs have grown massive and generate larger feedback energy. Thus, we find that BHs need to grow to $M_{\rm BH} > 10^5 M_\odot$, in order to suppress star-formation, even in these dwarf galaxies. BH feedback causes a reduction of SFR up to 5 times in the different runs.

The red curve (run *BHs2h1e6*) already quenches SF as early as $z \sim 8$. This is because the BH has already grown to $M_{\rm BH} \sim 5 \times 10^5 M_\odot$ at that epoch, more massive than all the other runs. As another example, the brown (run *BHs3h4e7*) and royal-blue (run *BHs3h5e7*) curves quench SF from $z \sim 4.5$ to $z \sim 3.5$. This is the epoch when the BH masses in these runs increase from $M_{\rm BH} = 10^5 M_\odot$ to $M_{\rm BH} = 10^6 M_\odot$.

4. Conclusions

We conclude that: (i) IMBHs at DG centers grow from $10^2 - 10^3 M_\odot$ to $10^5 - 10^6 M_\odot$ by $z \sim 4$ in a cosmological environment. These IMBHs in DGs can become the seeds of supermassive BHs (which grows to $M_{\rm BH} \sim 10^9 M_\odot$) in massive galaxies. (ii) Star formation is quenched when the BHs have grown to $M_{\rm BH} > 10^5 M_\odot$. We find a positive correlation between the mass growth BHs and the quenching of SF.

Acknowledgements. We are most grateful to Volker Springel for allowing us to use the GADGET-3 code. This work is supported by FAPESP (Jovem Pesquisador grant number 2016/01355-5). The numerical simulations were performed in the computing cluster GAPAE of the High Energy and Plasma Astrophysics group of IAG-USP.

References

Barai, P. et al. 2013, MNRAS, 430, 3213
Barai, P., Viel, M., Murante, G., Gaspari, M. & Borgani, S. 2014, MNRAS, 437, 1456
Barai, P., Monaco, P., Murante, G., Ragagnin, A. & Viel, M. 2015, MNRAS, 447, 266
Barai, P., Murante, G., Borgani, S., Gaspari, M., Granato, G. L., Monaco, P. & Ragone-Figueroa, C. 2016, MNRAS, 461, 1548
Bondi, H. 1952, MNRAS, 112, 195
Dashyan, G., Silk, J., Mamon, G. A., Dubois, Y. & Hartwig, T. 2017, eprint arXiv:1710.05900
Di Matteo, T., Khandai, N., DeGraf, C., Feng, Y., Croft, R. A. C., Lopez, J. & Springel, V. 2012, ApJ, 745, L29
Hahn, O. & Abel, T. 2011, MNRAS, 415, 2101
Hoyle, F. & Lyttleton, R. A. 1939, Proc. Cam. Phil. Soc., 35, 405
Marleau, F. R., Clancy, D., Habas, R. & Bianconi, M. 2017, A&A, 602, A28
Martin, C. L. 1999, ApJ, 513, 156
Penny, S. J. et al. 2017, submitted to MNRAS, eprint arXiv:1710.07568
Planck Collaboration; Ade, P. A. R. et al. 2016, A&A, 594, A13
Schaye, J. et al. 2015, MNRAS, 446, 521
Shakura, N. I. & Sunyaev, R. A. 1973, A&A, 24, 337
Silk, J. 2017, ApJ, 839, L13
Springel, V. & Hernquist, L. 2003, MNRAS, 339, 289
Springel, V. 2005, MNRAS, 364, 1105
Springel, V., Di Matteo, T. & Hernquist, L. 2005, MNRAS, 361, 776
Tornatore, L., Borgani, S., Dolag, K. & Matteucci, F. 2007, MNRAS, 382, 1050
Wiersma, R. P. C., Schaye, J. & Smith, B. D. 2009, MNRAS, 393, 99